An Application of the Hybrid Moment Method/Green's Function Technique to the Optimization of Resistive Strips

R. Craig Baucke
GE Aircraft Engines M/D J185
1 Neumann Way
Cincinnati, OH 45215-6301

Abstract - *An automatic method of synthesizing resistive tapers is developed. This method embeds a hybrid moment method/Green's function inside a nonlinear optimization package. Using this technique, resistive tapers are rapidly synthesized for complex scatterers which can consist of multiple resistive strips, as well as large, arbitrary conducting regions. The method is applied to the optimization of resistive tapers that reduce the diffraction from conducting scatterers.*

I. INTRODUCTION

Resistive strips are used in various applications to modify the electromagnetic scattering characteristics of an antenna or scatterer. They are used to reduce the diffraction from conductive edges or discontinuities [1-2], approximate an infinite ground plane [3], improve the performance of a compact range reflector [4], and attenuate energy in waveguide [5]. Even greater control over the scattering characteristics of the structure are obtained by tapering the value of the strip resistance [6,7].

While a physical-optics based method for synthesizing effective resistive tapers has been developed by Haupt [8], it is only applicable for a simple single strip geometry at E-polarization. The more general problem of defining optimum resistive tapers for multiple strips in the presence of arbitrary scatterers for arbitrary polarization is usually done in a trial and error fashion using established tapers as a starting point. The effectiveness of the proposed taper is computed using the method of moments (MoM or MM) or other numerical method (or measurements). While the trial and error approach to resistive taper design has led to a database of "good tapers", this approach is slow and may not result in the optimum taper, if one exists.

In this work, an automated method of synthesizing optimal resistive tapers is developed. Resistive tapers are computed in a minimum amount of

time within certain physical constraints. In effect, the trial and error method is replaced by a nonlinear optimization technique which searches for an optimal solution. The result is improved taper performance and drastically reduced design times. To implement this concept, the hybrid MM/Green's function (HMGF) technique described in [9] is applied to a moment method which analyzes two dimensional conductive and resistive strips at both E-polarization (TM_z) and H-polarization (TE_z). This approach is then encapsulated within a nonlinear optimization program such as [10, 11]. The resulting method rapidly computes the scattering levels from a number of different resistive tapers and searches for an optimum configuration within user defined constraints. This paper shows that the optimization of moment method analysis is only practical due to the application of the HMGF technique. In addition, the simultaneous optimization of a resistive taper for both polarizations is demonstrated, as well as the optimization of multiple tapers simultaneously.

II. Moment Method Approach

The choice of moment methods is critical to the efficiency of the optimization process. For E-polarization, an efficient Galerkin method developed by the author which utilizes pulse basis and pulse testing functions for metal and resistive scatterers is chosen. For H-polarization, the method of Liu and Balanis [12] has been enhanced to include resistive strips. This method uses pulse basis functions and thereby creates fictitious line charges at cell boundaries. In practice, the method of [12] provides fairly accurate far field results as long as the cell widths are about 1/10th of a wavelength. Since point matching is employed, it is very efficient.

Both the E-polarization and H-polarization moment methods use the electric field integral equation (EFIE). While the EFIE allows for the analysis of open structures such as resistive strips, interior resonances may exist for closed perfectly conducting (PEC) structures.

The EFIE for each moment method is developed by relating the incident electric field E^i to the total field E^t and the scattered field E^s by

$$E^i(x,y) = E^t(x,y) - E^s(x,y). \tag{1}$$

For resistive strips, the total field is defined as

$$E^t(x,y) = R(x,y)\, J(x,y) \tag{2}$$

where R is the surface resistance and J is the surface current density.

Substituting (2) into (1) and applying basis and testing functions yields

$$\langle E^i, B_m \rangle = \langle RJ_n P_n, B_m \rangle - \langle E^s, B_m \rangle \tag{3}$$

where P_n is the basis function for the nth source cell, B_m is the testing function for the mth test cell and J_n is the unknown current on the nth cell. The first inner product on the right side of (3) contains the resistive term, and is defined as

$$\Delta Z = \langle RJ_n P_n, B_m \rangle . \tag{4}$$

The term ΔZ is nonzero when the domains of the basis and testing functions overlap, and when the resistance of the source domain is nonzero.

Pulse basis and testing functions are applied for TM_z polarization. In this case,

$$\Delta Z = \langle RJ_n \Pi_n, \Pi_m \rangle \tag{5}$$

where Π is the pulse function. This expression is nonzero when m=n and contributes only to the diagonal terms of the moment matrix.

Pulse basis and point matching are applied for TE_z polarization. In this case,

$$\Delta Z = \langle RJ_n \Pi_n, \delta_m \rangle , \tag{6}$$

which is also nonzero only for diagonal elements of the matrix. Since (5) and (6) are nonzero only for diagonal elements of the moment matrices, when the resistances of the cells are modified, only the diagonal terms of the impedance matrix are changed, and only by a constant value. If other basis functions such are piecewise linear (triangular) or sinusoidal are chosen, ΔZ is nonzero for off-diagonal terms, and more matrix modification is required when resistance values are changed.

Once the basis and testing functions are applied, (3) reduces to a matrix equation Zx=B. At this point, the HMGF method is applied to the system matrix.

III. Application of Hybrid MM/Green's Function Technique

To apply the HMGF method, the scatterer is divided into two sections. One of the sections contains the portion of the scatterer where the resistance could be modified in the optimization process. This section will be referred to as scatterer 1 (or S1). The rest of the scatterer (the portion remaining unmodified) is called scatterer 2 (or S2). This is shown in figure 1.

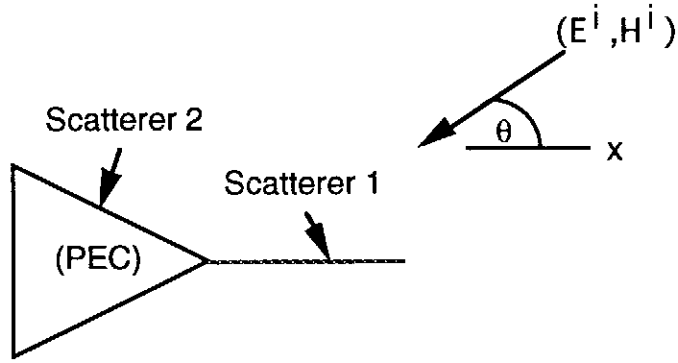

Figure 1. An example: scatterer 1 and scatterer 2.

In figure 1, S1 is a resistive sheet and S2 is a perfectly conducting closed triangular cylinder. The resistance of each cell on S1 may be modified while S2 will remain unchanged. The system matrix Z is partitioned as

$$Z = \begin{vmatrix} Z_{11} & Z_{12} \\ Z_{21} & Z_{22} \end{vmatrix} \tag{7}$$

where Z_{11} contains the matrix elements in which the observation and source points are located on S1, Z_{12} contains the elements in which the observation point is on S1 and the source point is on S2, Z_{21} contains the elements with the observation point on S2 and the source point on S1, and Z_{22} contains the elements with the observation and source points on S2. The order of Z_{11} is N_1 , where N_1 is the number of cells on S1, and the order of Z_{22} is N_2, where N_2 is the number of cells on S2.

Performing the linear algebra described in [9], the matrix equation is reduced from order $N_1 + N_2$ to order N_1 and reformulated as

$$(Z_{11} - Z_{12}Z_{22}^{-1}Z_{21})I_1 = B_1 - Z_{12}Z_{22}^{-1}B_2 \tag{8}$$

where B_1 is the excitation vector for S1, B_2 is the excitation vector for S2, and I_1 is the current solution for S1. The solution current on S2 can be found from

$$I_2 = Z_{22}^{-1}B_2 - Z_{22}^{-1}Z_{21}I_1 \tag{9}$$

The monostatic and bistatic scattering from the combination of S1 and S2 can be computed from the solution currents I_1 and I_2.

IV. Applying Nonlinear Optimization

In order to apply nonlinear optimization to this method, the echo width of the scatterer is computed by solving (8) with the initial (first guess) resistance values. This computation is three to four times slower than analyzing the entire scatterer with a traditional moment method approach, due to the computation of the complete Z_{22} inverse and several matrix multiplies. At this point, the inverse of the Z_{22} matrix is stored, as well as the Z_{12} and Z_{21} matrices. These matrices will not change in the following optimization iterations.

Once the initial resistive configuration is analyzed, the nonlinear optimizer computes new resistive values for the cells on S1. The system matrix in (8) is recomputed by subtracting and adding values to the appropriate diagonal terms. When the system in (8) is solved during subsequent iterations, the matrix fill time is very small and the solution time is drastically reduced compared to traditional moment methods. A comparison of the CPU time required for optimization of this method and a traditional moment method are shown in figure 2. These performance figures demonstrate the feasibility of performing nonlinear optimization on moment method calculations.

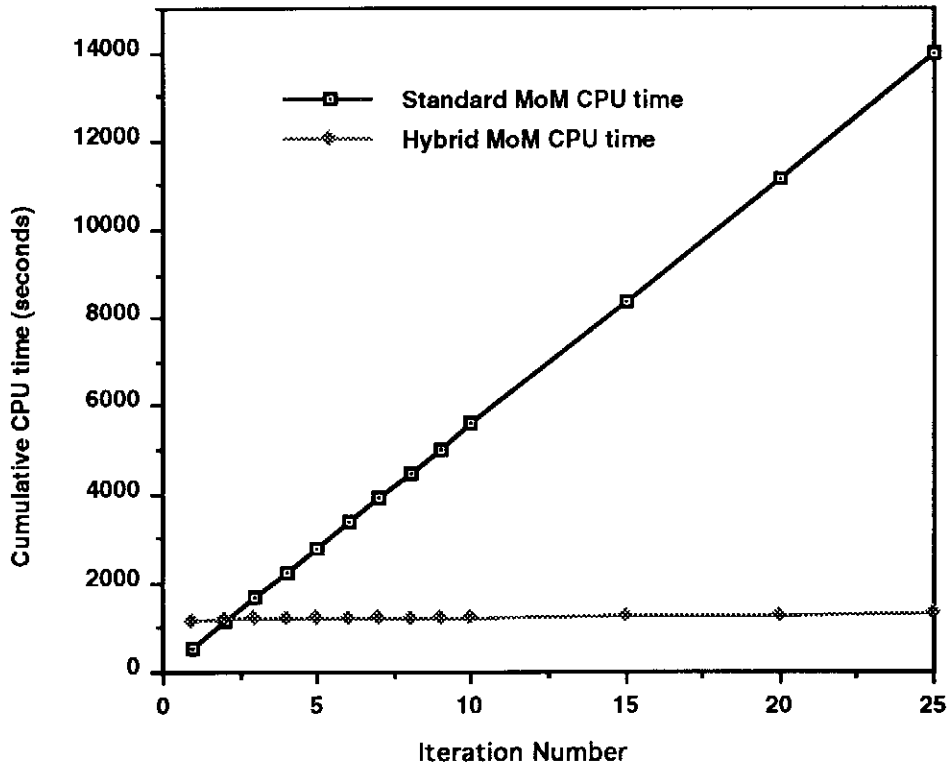

Figure 2. Comparison of the CPU time required for optimization with and without applying the HMGF technique.

The operation of the nonlinear optimizer requires the definition of a penalty function, which is the function to be minimized. While this function could be related to any quantity computed by the moment method (surface currents, near fields, etc.), in this case the penalty function F is defined as

$$F = \sum_{\alpha=1}^{2} \frac{1}{N_\theta} \sum_{i=1}^{N_\theta} \sigma^\alpha(\theta_i) \tag{10}$$

where α=1 is TM_z polarization, α=2 is TE_z polarization, N_θ is the number of monostatic angles, σ is the echo width in wavelengths, and θ_i is the ith monostatic angle. The function F is essentially a sector average of the echo width.

The optimizer attempts to minimize F by modifying the resistive values on S1. A flow chart of the optimization process is shown in figure 3.

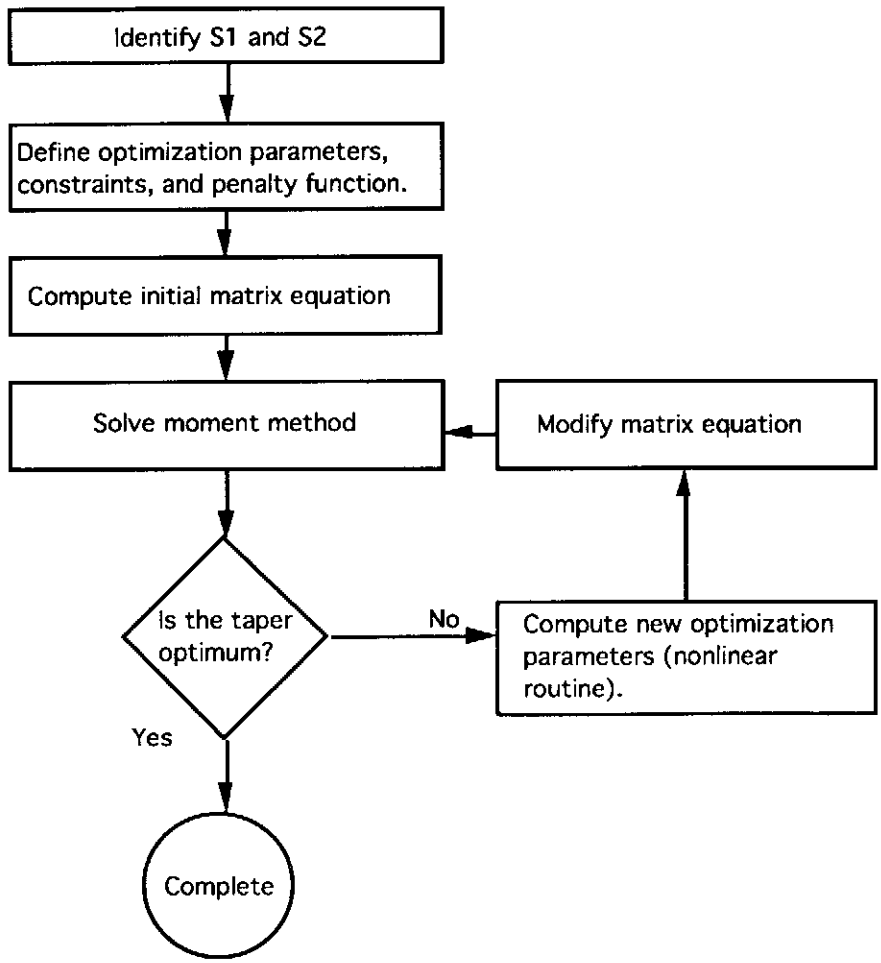

Figure 3. Flow chart of the resistive taper optimization process.

The choice of nonlinear optimization routines is limited by the type of function to be minimized. Since gradients of the function to be minimized in this work (10) are difficult to obtain, optimization methods which do not require explicit gradients are chosen. In addition, the resistance values of the cells are constrained to positive values that can be manufactured (it is difficult to accurately produce and measure resistive strips with resistances much greater than 3000 ohms/square). Thus, a constrained optimization is chosen.

In this work, the rotating coordinates method described in [10] and the Complex algorithm [11] are both applied. Both are direct search routines which utilize different search strategies. As in the case of all nonlinear optimizers, convergence to the absolute minimum is not guaranteed. To avoid nonoptimal local minima, the optimization process is carried out with different starting points and step sizes.

V. RESISTIVE TAPER OPTIMIZATION APPROACHES

The method developed in this paper is applied to the optimization of resistive tapers on S1 in two different fashions. In the first, the resistance value of each cell is an optimization parameter, while in the second approach the coefficients of a polynomial function are the parameters.

The first approach provides a very flexible approach to taper optimization, but often results in resistive tapers which cannot be constructed due to large fluctuations in the values of the resistances along the strips. These fluctuations in the optimal taper can be reduced by constraining the resistive values properly. However, it may still be difficult to create a smooth taper by optimizing in this fashion, and the effective bandwidth of the taper (the frequency range over which the taper has acceptable performance) may be small.

In the second approach, polynomial optimization, the nonlinear optimizer adjusts the coefficients of polynomials over each resistive taper in S1. For instance, if the user chooses a quadratic polynomial taper,

$$R(x) = ax^2 + bx + c \qquad (0 \le x \le 1), \tag{11}$$

coefficients a, b and c are modified by the optimizer. The variable x is the normalized distance along the strip.

The natural result of this optimization is a smooth taper (with the smoothness dependent on the order of the polynomial), as well as improved bandwidth. However, the performance at the frequency of optimization will probably be inferior to the first method. Thus, the first method is better for narrow band designs, and the second method is better for broadband designs. A comparison of the echo width and optimal taper computed by these two approaches for an example problem consisting of a flat resistive strip in front of a PEC is given in figures 4 and 5.

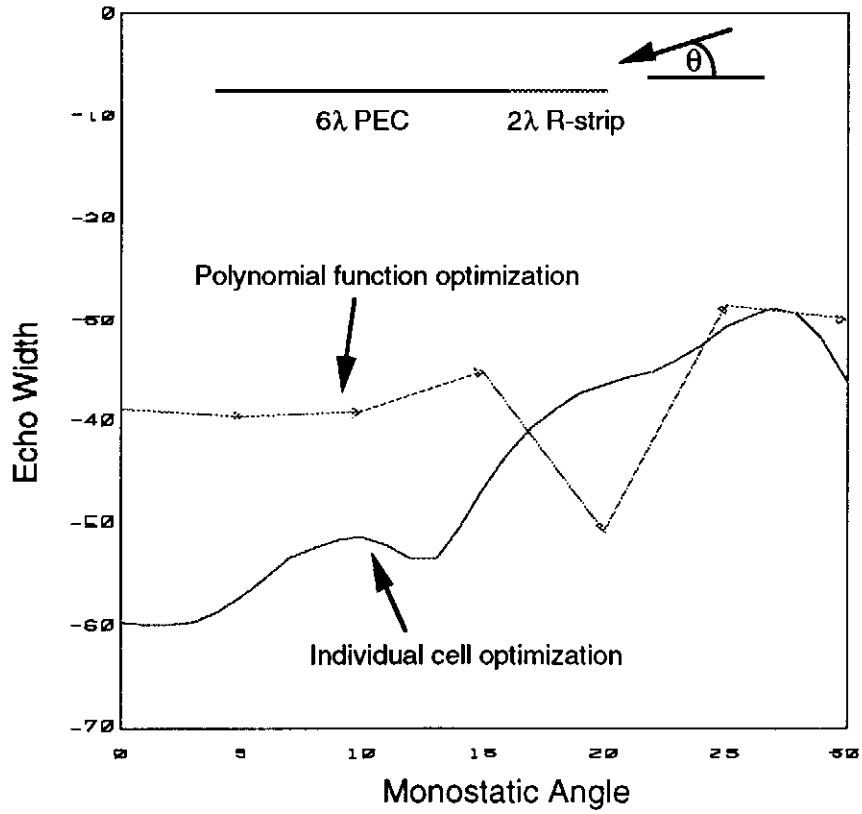

Figure 4. Comparison of echo width for resistive strip optimization using individual cell optimization and polynomial function optimization.

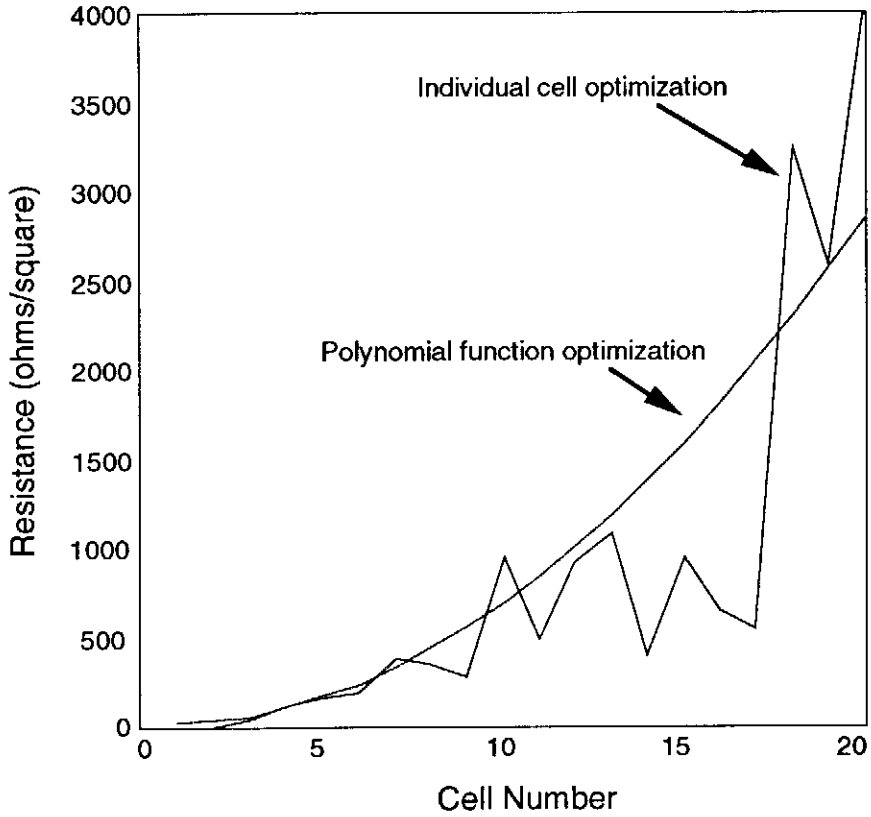

Figure 5. Comparison of resistive taper functions for resistive strip optimization using individual cell and polynomial function optimizations.

In figure 5, the optimal polynomial and individual cell values are shown as smooth and piecewise linear functions, respectively. In the context of the moment methods used in this work (5-6), the resistance of each cell is defined as a constant. Therefore, the functions in figure 5 are approximated by a set of step functions in the moment method discretization.

The first of two simple example problems is shown below.

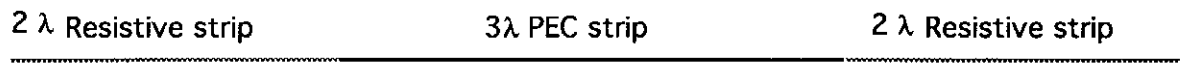

Figure 6. A single resistive strip scatterer.

In this problem, the leading and trailing resistive strips are optimized at both TM_z and TE_z polarizations using a quadratic taper that is constrained to resistive values between 3000 and 1 ohms/square. The initial values of each resistive strip are 200 ohms/square with no variation along the strips. The resistive strip scatterer S1 consists of 40 cells (20 cells on the leading edge and 20 cells on the trailing edge), and the metal scatterer S2 is divided into 30 cells. Figure 7 compares the echo widths of the optimized scatterer to the initial scatterer for TM_z and TE_z polarization. The penalty function in both problems is the average monostatic echo width of the scatterer from +30 to -30 degrees, sampled every 5 degrees.

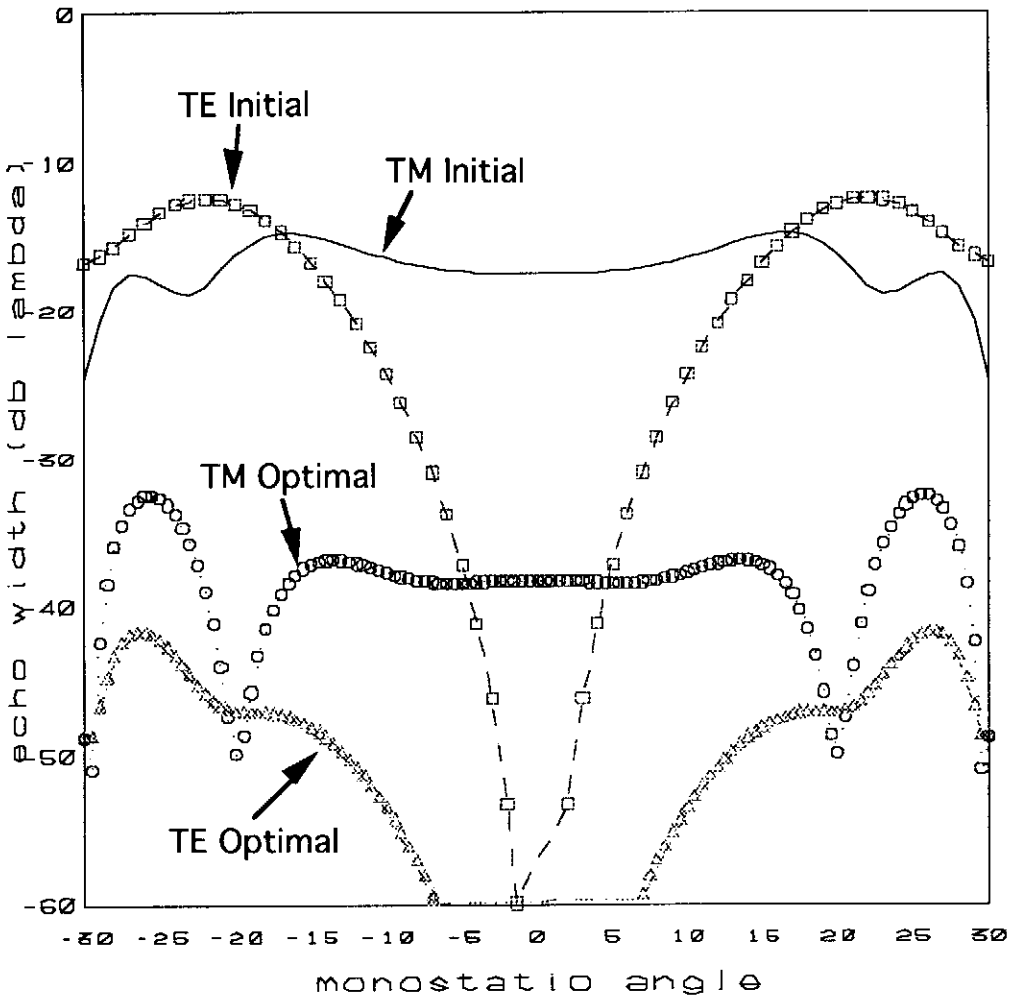

Figure 7. A comparison of the initial and optimized monostatic echo width from the scatterer in figure 6.

The resulting optimal quadratic taper on the leading edge strip is

(12) $R(x) = 3000x^2 + 131x + 6$

and the optimal taper on the trailing edge strip is

(13) $R(x) = 2778x^2 + 4x + 10.$

where the zero value of x in (12) and (13) is located at the junction of the corresponding resistive strip and PEC.

The optimization results in figure 7 require 496 iterations of the resistive values and 150 CPU seconds on a VAX 6510.

Both of the optimization techniques [10, 11] have been applied to this example, yielding nearly identical results. The results in figure 7 are obtained using the optimization method of [10].

In the second problem, another identical strip scatterer is placed 0.75 wavelengths above the original scatterer as shown in figure 8.

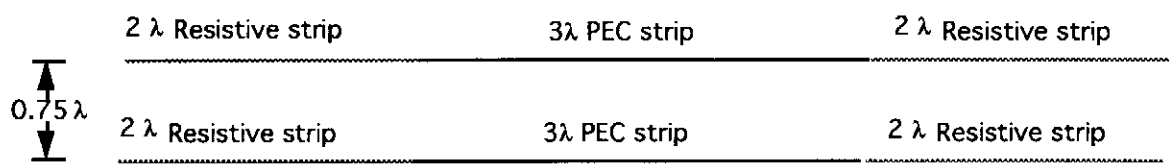

Figure 8. Two parallel resistive strips.

In the scatterer above, the four resistive strips making up S1 are divided into 80 cells and the PEC strips making up S2 consist of 60 cells. The same penalty function is used as in the previous example.

Figure 9 compares the echo widths of the optimized scatterer in figure 8 to the initial scatterer for TM_z and TE_z polarization.

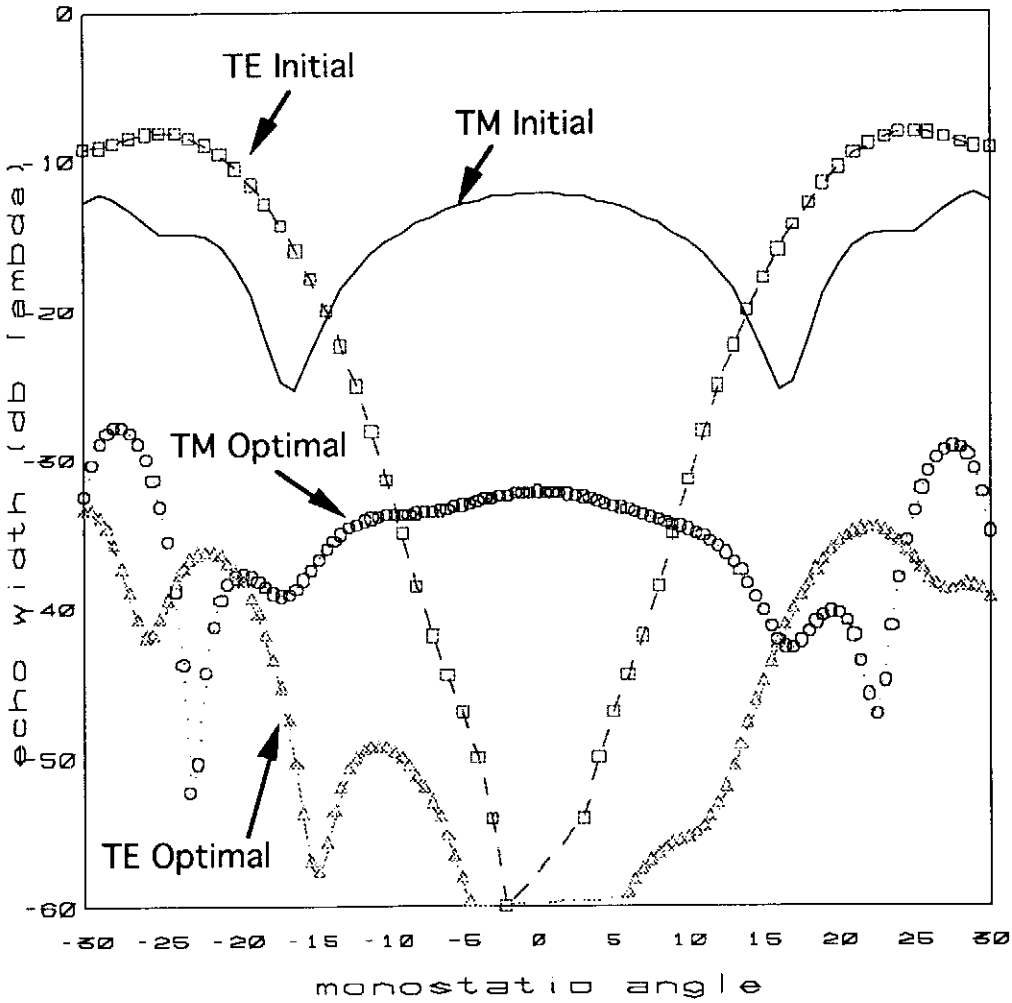

Figure 9. A comparison of the initial and optimized monostatic echo width from the scatterer in figure 8.

The resulting optimal quadratic taper on the leading edge strips are

(14) $R(x) = 3000x^2 + 4x + 1$ (upper)
$R(x) = 2990x^2 + 4x + 3$ (lower)

and the optimal taper on the trailing edge strips are

(15) $R(x) = 1975x^2 + 12x + 12$ (upper)
$R(x) = 1065x^2 + 14x + 4$ (lower).

The optimization results in figure 9 require 430 iterations of the resistive values and 534 CPU seconds on a VAX 6510.

VII. CONCLUSIONS

In this work, an automatic method of synthesizing optimum resistive tapers for multiple arbitrary resistive strips in any scattering environment has been developed. The optimization is performed simultaneously for both TE_z and TM_z polarizations. The results of individual cell and polynomial function optimization are demonstrated and compared. The efficiency of this method due to the application of the HMGF technique is shown. While two dimensional results are shown here, this method could be easily applied to a three dimensional moment method structure.

REFERENCES

[1] T.B.A. Senior, "Scattering by resistive strips," *Radio Science,* vol. 14, no. 5, Sept.-Oct. 1979, pp. 911-924.

[2] M.C. Heaton, "Electromagnetic scattering from impedance strips and impedance-loaded conducting strips," Master's Thesis, Air Force Institute of Technology, Dec. 1990.

[3] G.F. Herrmann, "Numerical Computation of Diffraction Coefficients," *IEEE Trans. Antenna Propagat.*, vol. 35, no. 1, January 1987, pp. 53-61.

[4] P.A. Beyerle, I.J. Gupta and E.H. Newman, "Compact range reflectors with resistive strip terminations - TM case," Ohio State University Technical Report 721223-5, Sept. 1989.

[5] I.M. Braver, P. Sh. Fridberg and K.L. Garb, "Frequency-independent waveguide attenuator with a resistive film in the diagonal plane," *Microwave Journal,* Nov. 1990, pp. 179-182.

[6] T.B.A. Senior and V.V. Liepa, "Backscattering from Tapered Resistive Strips, " *IEEE Trans. Antenna Propagat.*, vol. 32, no. 7, July 1984, pp. 747-751.

[7] R.L. Haupt and V.V. Liepa, "Resistive tapers that place nulls in the scattering patterns of strips," *IEEE Trans. Antennas Propagat.*, vol. 38, no. 7, July 1990, pp. 1117-1119.

[8] R.L. Haupt and V.V. Liepa, "Synthesis of tapered resistive strips, " *IEEE Trans. Antenna Propagat.*, vol. 35, no. 11, Nov. 1987, pp. 1217-1225.

[9] E.H. Newman, "An overview of the hybrid MM/Green's function method in electromagnetics, " *Proceedings of the IEEE.*, March 1988, pp. 270-282.

[10] H.H Rosenbrock, "An Automatic Method for finding the Greatest or Least Value of a Function, " *Computer Journal*, vol. 3, October 1960, pp. 175-184.

[11] P.E. Gill, W. Murray and M.H. Wright, *Practical Optimization*, Academic Press, New York, 1981.

[12] K. Liu and C.A. Balanis, "Simplified formulations for two-dimensional TE-polarization field components, " *IEEE Trans. Antenna Propagat..*, vol. 39, no. 2, February 1991, pp. 259-262.